

# Dimeric Cationic Amphiphilic Polyproline Helices for Mitochondrial Targeting

Iris M. Geisler · Jean Chmielewski

Received: 18 February 2011 / Accepted: 24 May 2011 / Published online: 7 June 2011  
© Springer Science+Business Media, LLC 2011

## ABSTRACT

**Purpose** Efficient delivery of therapeutic biopolymers across cell membranes remains a daunting challenge. The development of cell-penetrating peptides (CPPs) has been useful; however, many CPPs are found trapped within endosomes, limiting their use as delivery agents. We optimize a class of CPPs, cationic amphiphilic polyproline helices (CAPHs), for direct transport into cells with mitochondrial localization through dimerization.

**Methods** The CAPH P11LRR used for this study has been found to enter cells by two distinct pathways: an endocytotic pathway was favored at low concentrations; internalization by direct transport was observed at higher concentrations. CAPH was dimerized to probe if direct transport within cells may be enhanced through increased association of CAPH with the membrane and through the association of individual peptides within the membrane.

**Results** The dimerization of the CAPH was found to significantly increase cellular uptake over its monomeric counterpart, with a concomitant lowering of the concentration threshold favoring direct transport. Evidence for direct transport within cells and mitochondrial localization was observed.

**Conclusions** CAPH cellular uptake efficiency can be significantly enhanced through peptide dimerization while favoring cell entry via direct transport at low concentration with low cell toxicity.

**KEY WORDS** cationic amphiphilic polyproline helices · cell penetrating peptides · dimerization · mitochondrial targeting

**Electronic supplementary material** The online version of this article (doi:10.1007/s11095-011-0493-7) contains supplementary material, which is available to authorized users.

I. M. Geisler · J. Chmielewski (✉)  
Department of Chemistry, Purdue University  
560 Oval Drive  
West Lafayette, Indiana 47907, USA  
e-mail: chml@purdue.edu

## ABBREVIATIONS

CAPH	cationic amphiphilic polyproline helix
CPP	cell-penetrating peptide
FBS	fetal bovine serum
FCCP	carbonylcyanide p-trifluoromethoxyphenylhydrazone
FL	fluorescein
Fmoc	9-fluorenylmethyloxycarbonyl
HATU	N,N,N',N'-Tetramethyl-O-(7-azabenzotriazol-1-yl) uranium hexafluorophosphate
MTT	3-(4,5-dimethylthiazol-2-yl)-2,5-diphenyltetrazolium bromide
NHS-FL	5-(and 6)-carboxyfluorescein, succinimidyl ester
PBS	phosphate-buffered saline

## INTRODUCTION

Over the past two decades, the discovery of cell-penetrating peptides (CPPs) has generated many advances toward efficient cellular delivery of membrane-impermeable drugs. Generally, CPPs are described as a class of short peptide sequences that are rich in basic amino acids and able to deliver a variety of bioactive molecules across membranes of different cell lines with high efficiency and minimal toxicity (1). Some CPPs also feature an alternating pattern of charged, polar amino acids and hydrophobic, non-polar amino acids, rendering an overall amphiphilic peptide (2–12). CPPs have been found to deliver a range of cargo into cells, from proteins and oligonucleotides to magnetic nanoparticles (13–16). To date, over 30 different CPPs have been developed and studied, including nuclear localization sequences (17), polylysine and polyarginine peptides (18),  $\beta$ -peptides (3,19), peptoids (20), loligomers (21), oligocarbamates (22), PNA oligomers (23) and polyproline helices (2,4,24,25).

The mechanism of cellular uptake for CPPs remains a widely discussed subject, with most studies focusing on the Tat peptide (Tat<sub>p</sub>; FL-YGRKKRRQRRR-NH<sub>2</sub>). Thus far, two distinct mechanisms of internalization, namely endocytosis and direct transport, have been observed for the internalization of various CPPs (1,26). Although endocytosis has generally been acknowledged as the major mode of uptake for Tat<sub>p</sub> and Tat<sub>p</sub> conjugates, distinct uptake mechanisms are evident in different systems, with some indicated to be cell-type and cargo-specific. A direct transport mechanism of cell entry is advantageous overall, as internalization of the CPP and its cargo would avoid endosomes, thereby increasing the possibility of direct sub-cellular localization.

Previously, a CPP was described (P11LRR—Fig. 1) that enters cells via two distinct mechanisms depending on the concentration used (12). Treatment of cells with P11LRR at concentrations of <10 μM demonstrated that an endocytotic pathway was favored, as the peptide was observed to co-localize with a LysoTracker dye. At concentrations >20 μM of P11LRR we observed a shift in sub-cellular localization to the mitochondria and hypothesized that internalization by direct transport occurred, as opposed to endocytotic uptake followed by release from the endosome. This hypothesis was confirmed by visualizing mitochondrial sub-cellular localization of P11LRR at very early time points after incubation with cells. The observed direct transport of P11LRR at higher concentrations was proposed to be a result of enhanced association of CAPHs within the membrane (12), potentially through pore-forming mechanisms such as the barrel stave (27) and toroidal models (28) of association. In addition, mitochondrial localization through direct transport with P11LRR was found to be driven by the mitochondrial membrane potential (12).

Besides mechanistic considerations, the intriguing mitochondrial targeting properties of the CAPH monomer at high concentrations prompted us to more closely investigate its potential as a mitochondria-specific targeting agent. The structural features of compounds that are known to accumu-

late within the mitochondria include sufficient lipophilicity, along with delocalized positive charges within the molecule (29). The positive charge of guanidinium groups is believed to aid the interaction with the mitochondrial membrane due to the high membrane potential of the negatively charged membrane facing the cytosol (30). Other investigators have made similar observations in regards to the role of lipophilicity in mitochondrial localization (31–33).

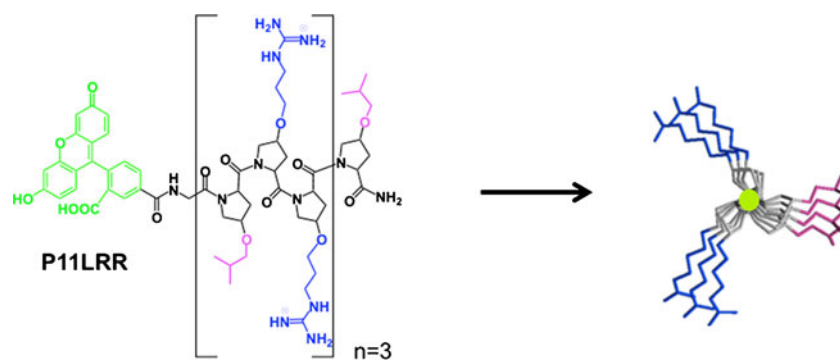
Although most CPPs reported in the literature are monomeric, some examples of multimeric CPPs have been described (34–37). In one study, Tat<sub>p</sub> was tetramerized, and a correlation between CPP valency and cellular uptake efficiency was observed (37). Likewise, the oligomerization of CPPs, such as Tat, Hp-1, Antp and H4, into branched dimers, tetramers and octamers was shown to significantly enhance the cellular uptake of adenovirus (36). These examples clearly highlight the beneficial effects of peptide oligomerization in regard to cell uptake with CPPs. Herein, we discuss the dimerization of the CAPH P11LRR to probe if direct transport within cells may be enhanced through increased association of the CAPH with the membrane and through the association of individual peptides within the membrane, potentially resulting in more effective mitochondrial targeting at a lower CAPH threshold. The uptake efficiency and sub-cellular localization of three different CAPH dimers were investigated and compared to their monomeric counterpart.

## MATERIALS AND METHODS

### Materials

Rink amide AM (200–400 mesh, 0.71 mmol/g) resin, Fmoc-Glycine-OH, Fmoc-β-alanine-OH, Fmoc-4-aminobutyric acid and N-(9-fluorenylmethoxycarbonyloxy)succinimide (Fmoc-OSu) were purchased from Advanced ChemTech and/or Novabiochem. Z-Hyp-OH (N-Cbz-Hydroxy-L-proline) was purchased from ChemImpex. NHS-Fluorescein was purchased from Pierce Thermo

**Fig. 1** The structure of CAPH monomer P11LRR with a representative cartoon looking down the helix (right). Hydrophilic residues are shown in blue, hydrophobic residues are shown in pink, fluorophore attachment is indicated by the green sphere.



Scientific. Reagents for the synthesis of the modified proline amino acids and peptide linker were obtained from Aldrich. HATU was obtained from Oakwood Products. RPMI 1640, penicillin-streptomycin, L-glutamine, trypsin and 4-well LabTek confocal dishes were purchased from VWR. LysoTracker Red and MitoTracker Red CMXRos were purchased from Invitrogen. MCF-7 cells were purchased from ATCC.

## Methods

### Synthesis of Dimer Linker C5

For detailed synthetic protocols for the preparation of the linker C5, please refer to the [Supplementary Material](#). Briefly, the dimer linker was prepared from commercially available pentanediol over five steps. First, pentanediol was mono-protected with TBDMS, and the residual hydroxyl group was oxidized to an aldehyde. Reductive amination of this aldehyde with commercially available 5-aminopentanol yielded the intermediate amine linker that was TBDMS deprotected and Fmoc protected at the secondary amine. In a final step, the dimer precursor was oxidized to yield the desired Fmoc protected di-carboxylic acid linker C5.

### Synthesis of Fluorescently Labeled CAPH Peptides

The P11LRR-FL CAPH was prepared on the Rink amide resin using Fmoc-based solid phase chemistry as previously described (2). CAPH P10LRR for use in dimer synthesis was prepared in the same manner and kept on solid support for dimerization. Briefly, P10LRR on Rink amide resin was treated with either Fmoc-glycine (Fmoc-Gly), Fmoc- $\beta$ -alanine (Fmoc- $\beta$ -Ala) or Fmoc-4-aminobutyric acid (Fmoc-ABUA) spacers and HATU as the coupling reagent. The Fmoc-protecting group was removed followed by addition of dimer linker C5 and HATU to dimerize P10LRR on resin. The Fmoc-protecting group was removed from the linker, and the resulting secondary amine on resin was reacted with Fmoc-glycine and HATU, followed by Fmoc-deprotection and NHS-fluorescein labeling. The dimeric CAPHs were simultaneously de-protected and cleaved from the resin using a trifluoroacetic acid (TFA) cocktail solution (95% TFA, 2.5% triisopropylsilane, 2.5% H<sub>2</sub>O). The crude peptides were purified to homogeneity by reverse-phase HPLC using a linear 60 min gradient of a solvent system consisting of solvent A (acetonitrile or methanol with 0.1% TFA) and solvent B (water/0.1% TFA) with a flow rate of 10 mL/min ( $\lambda_{214}$  nm and  $\lambda_{254}$  nm). All peptides were characterized by matrix-assisted laser desorption ionization mass spectrometry (MALDI), and final stock solutions were quantified by UV-vis analysis. MALDI data: P11LRR calculated MW 2382.8, observed 2383, (P10LRR-Gly)<sub>2</sub>-

C5-G-FL calculated MW 4642, observed 4640, (P10LRR- $\beta$ -Ala)<sub>2</sub>-C5-G-FL calculated MW 4670, observed 4670, (P10LRR-ABUA)<sub>2</sub>-C5-G-FL calculated MW 4698, observed 4698. All peptides and dimers were found to be greater than 97% pure by analytical HPLC.

### Flow Cytometry

MCF-7 cells were seeded into 24-well plates at a density of 100,000 cells/well in 0.5 mL of RPMI 1640 media supplemented with 10% FBS, 100 units/mL penicillin and 0.1 mg/mL streptomycin and L-glutamine and grown in a humidified 5% CO<sub>2</sub> atmosphere at 37°C for 48 h. Cells were incubated with 2.5  $\mu$ M of monomeric and dimeric CAPHs (prepared in sterile de-ionized water) for 1, 3 and 5 h in serum-free RPMI 1640 media (190  $\mu$ L/well). Following incubation, cells were washed three times with 100  $\mu$ L/well PBS (Ca<sup>2+</sup> and Mg<sup>2+</sup>-deficient phosphate-buffered saline). The cells were gently dislodged from the wells with 100  $\mu$ L of trypsin (0.25%) per well, re-suspended in 300  $\mu$ L of fresh culture medium, transferred to culture tubes and kept on ice prior to analysis. Untreated cells were also analyzed to determine background fluorescence levels. Mean fluorescence values were measured on a BD FACS Calibur Flow Cytometer using an air-cooled laser for excitation of fluorescein at 488 nm.

### Laser Scanning Confocal Microscopy (LSCM)

MCF-7 cells were seeded at a density of 50,000 cells/well into four-chambered LabTek dishes in 1 mL of complete RPMI 1640 culture media and grown in a humidified 5% CO<sub>2</sub> atmosphere at 37°C for 48 h. Cells were treated with each CAPH for 1 h at a concentration of 2.5  $\mu$ M (or 500 nM for 4 h) in 400  $\mu$ L of serum-free RPMI 1640 culture media. Following incubation, the cells were washed three times with 100  $\mu$ L PBS, re-suspended in 300  $\mu$ L of fresh culture medium and imaged immediately. For co-staining experiments, MCF-7 cells were first treated with each of the CAPHs under the above conditions, followed by incubation with either 400 nM LysoTracker Red or 200 nM MitoTracker Red in 400  $\mu$ L of serum-free RPMI 1640 culture medium for 30 min. Cells were washed and re-suspended in 300  $\mu$ L fresh culture medium for immediate imaging as described above. For mechanistic investigations, cells were pre-incubated with either 1  $\mu$ M FCCP or 1  $\mu$ M gramicidin in 400  $\mu$ L of serum-free RPMI 1640 medium for 1 h, followed by the same treatment of cells as mentioned above. Live cells were imaged on an inverted confocal fluorescence microscope (Olympus, FV1000) equipped with a 60x oil immersion objective (Numerical aperture 1.2). A 488-nm Ar<sup>+</sup> laser was used to excite the fluorescently labeled CAPHs. A 543-nm HeNe laser was

used for the excitation of LysoTracker and MitoTracker Red. To eliminate fluorescence bleed-through, multicolor images were obtained using high-speed frame sequential imaging. All images were obtained at identical settings to allow for direct comparison.

### MTT Cell Viability Assay

Cellular toxicity of the oligomeric CAPHs was examined using the 3-(4,5-dimethylthiazol-2-yl)-2,5-diphenyltetrazolium bromide (MTT) cell viability assay. MCF-7 cells were seeded into 96-well plates at a density of 10,000 cells/well in 100  $\mu$ L of RPMI 1640 media and grown in a humidified 5% CO<sub>2</sub> atmosphere at 37°C for 24 h. The cells were then incubated for 4 h in the presence of fluorescently labeled and non-fluorescent CAPHs at peptide concentrations of 1 and 5  $\mu$ M in 60  $\mu$ L serum-free RPMI 1640 culture media per well. Following peptide incubation, 20  $\mu$ L of 5 mg/mL of MTT (in PBS, pH 7.4) was added to each well, and the cells were incubated for an additional 1.5 h. The MTT solution was then removed, and the precipitated formazan crystals were dissolved in 200  $\mu$ L of DMSO each. The absorbance of each well was read with a TECAN SPECTRAFluor Plus fluorescence plate reader at 590 nm. For each experiment, a control of cells that were not incubated with any of the peptides was also analyzed. All samples were run in triplicate. The average absorbance for each sample was calculated and percent viability was determined using the following equation: % cell viability =  $A_{590}$  treated cells /  $A_{590}$  untreated cells  $\times$  100.

## RESULTS AND DISCUSSION

### Design of CAPH Dimers

The CAPH P11LRR contains both a hydrophobic face composed of four isobutyl groups, and a hydrophilic face containing six positively charged guanidinium groups (Figs. 1 and 2a—P<sub>L</sub> and P<sub>R</sub>, respectively). Dimerization of this CAPH provides the opportunity to probe if direct transport within cells may be enhanced through increased association of the CAPH with the negatively charged cell membrane due to the increased overall charge of the CAPHs and to determine if more efficient direct transport results in mitochondrial targeting at a lower CAPHs threshold. Although P11LRR has not been found to associate in aqueous solution, the concentration dependence of direct transport has been proposed to be due to increased CAPHs association within the membrane at higher concentrations (12). By crosslinking P11LRR, pre-associated dimeric forms of CAPHs would be generated that could also probe the effect of CAPH association on direct transport and mitochondrial targeting.

With these hypotheses in mind, an appropriate cross-linking strategy for P11LRR was designed (Fig. 2). Three different length spacers were devised to be directly attached to the N-terminus of the CAPH on resin: Fmoc-Gly, Fmoc- $\beta$ -Ala and Fmoc-ABUA (Fig. 2a—dimer spacers). A central linking moiety (Fig. 2a—dimer linker C5) was designed with two terminal carboxylic acids to attach two spacer-modified CAPHs on resin, with the inclusion of an internal secondary amine for fluorophore addition. Through molecular modeling, these spacer/linker combinations were found to be the most favorable to allow for association of the hydrophobic faces within the dimerized CAPHs (Fig. 2b). In the end, three fluorescently labeled CAPH dimers with varying spacer lengths, featuring 12 guanidinium groups and 8 hydrophobic residues each were designed: (P10LRR-Gly)<sub>2</sub>-C5-G-FL, (P10LRR- $\beta$ -Ala)<sub>2</sub>-C5-G-FL, (P10LRR-ABUA)<sub>2</sub>-C5-G-FL.

### Synthesis of CAPH Dimers

The unnatural amino acids and monomeric CAPHs were synthesized as previously described (2). To construct the CAPH dimers, P10LRR was synthesized on resin followed by the addition of either Fmoc-Gly, Fmoc- $\beta$ -Ala or 4-ABUA as the spacer (Fig. 1a). After Fmoc-deprotection, dimerization was performed on resin using the dimer linker C5. Following dimerization and Fmoc-deprotection, an Fmoc-glycine residue was added to the amine of linker C5, followed by Fmoc-deprotection and fluorescent labeling with NHS-fluorescein. The final peptides were cleaved from the resin, purified to homogeneity by reverse phase HPLC and characterized by MALDI mass spectrometry.

### In Cyto Uptake Efficiency of CAPH Dimers

When initially evaluated for efficiency of cell penetration, P11LRR and Tat<sub>p</sub> were investigated at a concentration of 50  $\mu$ M for 6 h, and P11LRR was found to enter cells about an order of magnitude more effectively than the Tat<sub>p</sub> peptide. We hypothesized that dimerization of P11LRR would allow us to work at significantly lower CAPH concentrations in shorter time periods. With this in mind, we studied the penetration of P11LRR and Tat<sub>p</sub> versus the dimeric CAPHs (P10LRR-Gly)<sub>2</sub>-C5-G-FL, (P10LRR- $\beta$ -Ala)<sub>2</sub>-C5-G-FL and (P10LRR-ABUA)<sub>2</sub>-C5-G-FL into MCF-7 breast cancer cells by flow cytometry at a concentration of 2.5  $\mu$ M for a period of 1, 3 or 5 h (Fig. 3).

The data obtained demonstrated that the cellular internalization efficiency of all CAPH dimers was significantly enhanced in comparison to their monomeric counterpart and Tat<sub>p</sub> (Fig. 3). Uptake was further increased with longer incubation times, however, not significantly. P10LRR-Gly)<sub>2</sub>-C5-G-FL, the dimer containing the shortest overall linkage

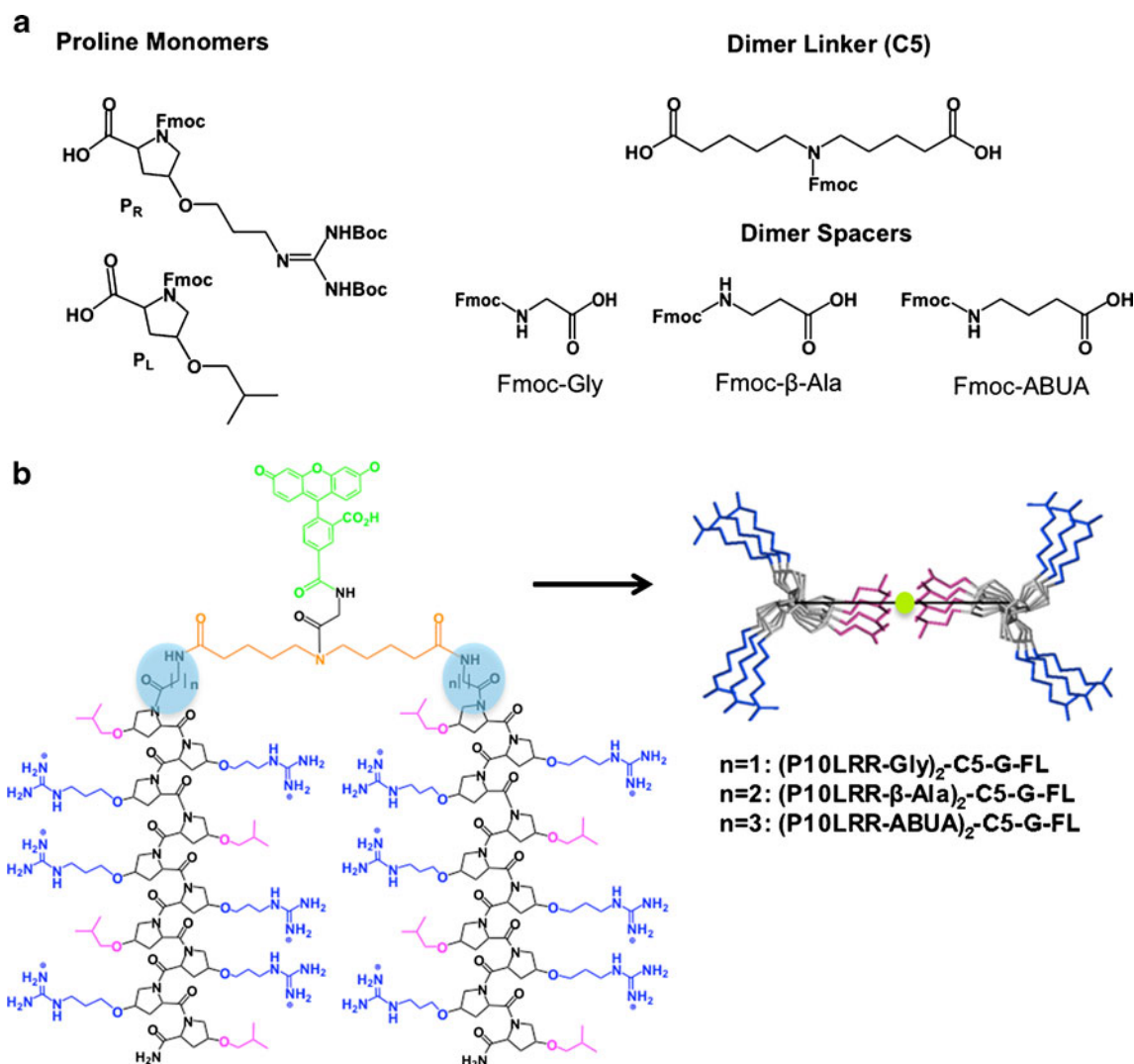


**Fig. 2** (a) The structures of proline monomers use for the CAPH synthesis, dimer linker (C5) and dimer spacers. (b) The structures of the CAPH dimers with a representative cartoon of the dimer (right); hydrophilic residues are shown in blue, hydrophobic residues in pink, fluorophore attachment indicated by the green sphere.

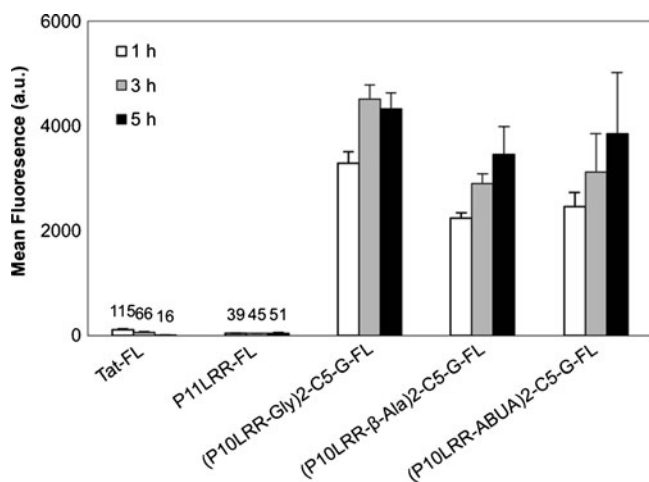


**Fig. 3** Cellular uptake of CAPH monomer P11LRR and dimers in MCF-7 cells after 1, 3 and 5 h of incubation with 2.5 μM of peptide, with comparison to Tat<sub>p</sub>.

(Gly+C5), was overall more efficiently internalized in comparison to the other two dimers. The overall difference in cell entry efficiency between dimers, however, was not dramatic, with increases in the range of 20 to 40%. These data indicate that linker distance is not a crucial factor for optimal cell penetration. In contrast to monomeric P11LRR and Tat<sub>p</sub>, the uptake efficiency of the dimers was far superior. After just 1 h of incubation the most potent CAPH dimer [(P10LRR-Gly)<sub>2</sub>-C5-G-FL] was internalized about 30-fold and 90-fold more effectively as compared to Tat<sub>p</sub> and P11LRR, respectively.

Electrostatic interactions of CPPs with proteoglycans, such as heparin sulfate, of the cell membrane are commonly considered the first step in peptide internalization (7,38), followed by subsequent peptide internalization. The hydrophobic character of CPPs, however, may also

allow the peptides to partition into the membrane's lipid bilayer as is observed for amphiphilic antibacterial peptides (39). The enhanced uptake efficiency of the CAPH dimers, therefore, could be a result of additional positive charges displayed on the surface of the polyproline helix, in addition to the increase in hydrophobic content of the dimers. For instance, it has been demonstrated that CPPs with more than six positive charges are more efficiently internalized, while CPPs with less than six charges were found to be significantly less effective (40).

CAPHs contain some structural features in common with antimicrobial peptides, such as a helical conformation (polyproline type II *versus* alpha or  $3_{10}$ ), cationic residues and an overall amphiphilic structure. Antimicrobial peptides have been shown to commonly enter cells via direct transport mechanisms, including pore forming mechanisms that are partly driven by the association of individual peptides within the membrane (39). The hydrophobic region of the amphiphilic peptides interact with the inner membrane lipids, while the hydrophilic region of the peptides forms the interior of the pore. The enhanced cellular uptake of the dimeric CAPHs may be due to such direct transport mechanisms, and further experiments to determine the subcellular localization of the dimers were performed to confirm this.

#### Sub-cellular Localization of CAPH Dimers

Since sub-cellular localization can be an indication of the route of peptide entry (direct transport *vs.* endocytosis), the

cellular fate of CAPH dimers was evaluated. MCF-7 cells were first treated with  $2.5 \mu\text{M}$  of each dimer for 1 h and were then analyzed by confocal microscopy. Confocal imaging revealed CAPH internalization in the form of punctuate fluorescence within cells (Fig. 4). Punctuate fluorescence is most often an indication of entrapment of fluorescent material within cytosolic vesicles (41), but may also be an indication of peptide localization to the mitochondria. Since endosomal/lysosomal localization is usually the most common cause for the occurrence of punctuate fluorescence, a co-staining experiment using LysoTracker Red was performed. To this end, MCF-7 cells were treated with  $2.5 \mu\text{M}$  of the CAPH dimers for a period of 1 h, followed by a washing step with PBS and incubation of the cells for an additional 30 min with LysoTracker Red. Live cell imaging was performed immediately thereafter. As the images indicate, no co-localization of CAPH dimers (green) and LysoTracker Red stain was observed in the overlaid images (Fig. 4). Hence, the observed punctuate fluorescence of the dimers within MCF-7 cells is not due to entrapment of peptide within endosomal/lysosomal compartments.

Since punctuate fluorescence can also arise from mitochondrial localization, a co-staining experiment using MitoTracker Red was performed to aid further investigations. Again, MCF-7 cells were treated with the CAPH dimers as described above, followed by a 30 min incubation with MitoTracker Red. The resulting images revealed a high level of co-localization of all CAPH dimers with MitoTracker Red (Fig. 5), corroborating the association of

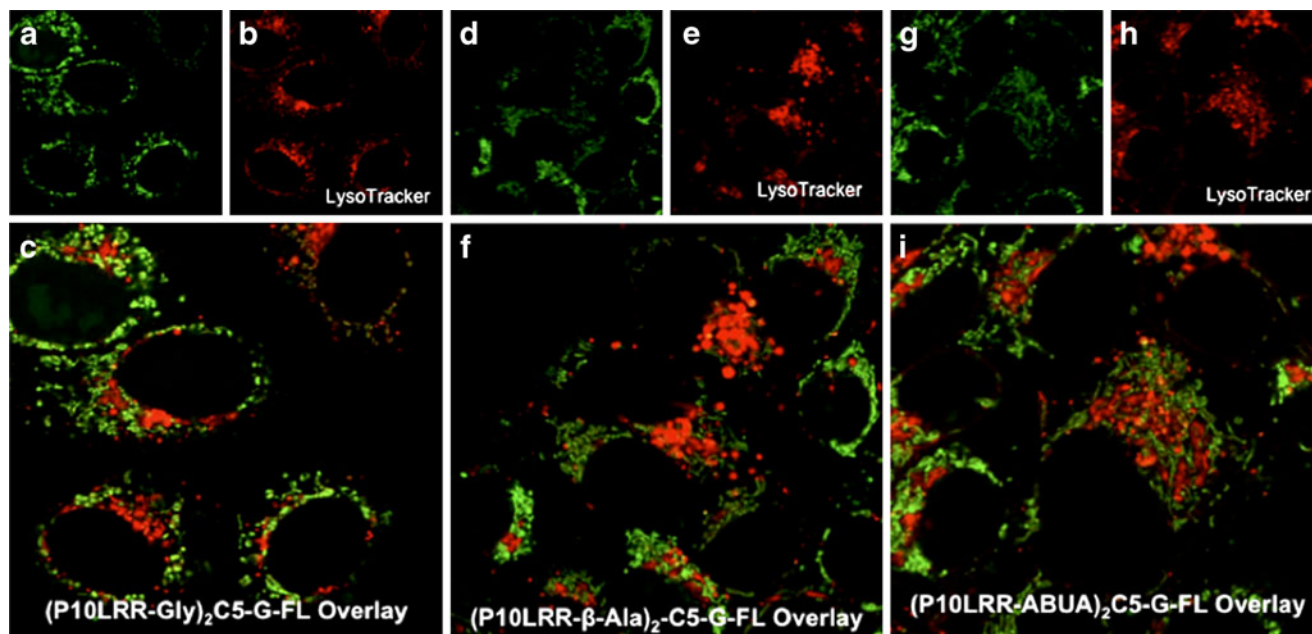


**Fig. 4** Confocal images of CAPH dimer internalization in MCF-7 cells after a 1 h incubation with  $2.5 \mu\text{M}$  of peptide (green channel) (a, d, g), LysoTracker images (red channel) (b, e, h) and the overlay images of CAPH dimers (green channel) with LysoTracker red (red channel) (c, f, i). ( $60\times$  objective with an additional  $3\times$  digital zoom).

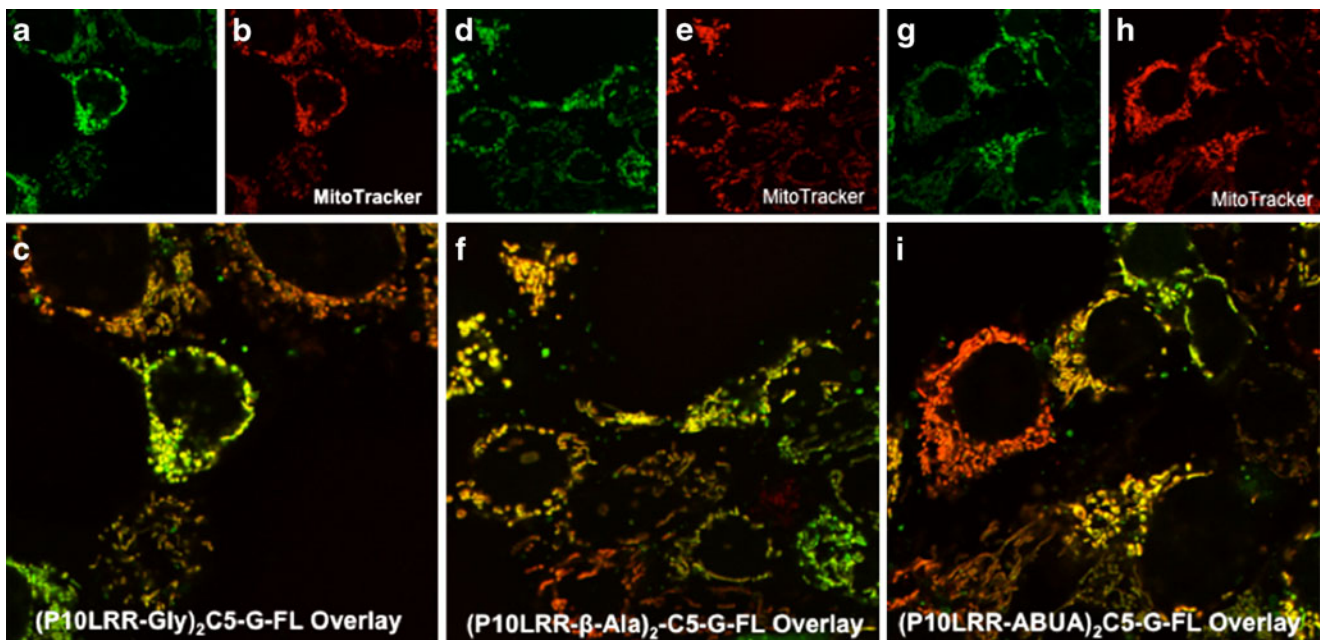


**Fig. 5** Confocal images of CAPH dimer internalization in MCF-7 cells after a 1 h incubation with  $2.5 \mu\text{M}$  of peptide (green channel) (**a, d, g**), MitoTracker images (red channel) (**b, e, h**) and the overlay images of CAPH dimers (green channel) with MitoTracker red (red channel) (**c, f, i**). ( $60\times$  objective with an additional  $3\times$  digital zoom).

the CAPH dimers with the mitochondria. These results demonstrate the mitochondrial targeting properties of all CAPH dimers at significantly lower concentration than we had previously observed with the CAPH monomer (12).

In order for the CAPH dimers to associate with mitochondria, the peptides need to move freely inside the cytoplasm. Two probable pathways allowing for internalization of peptide into the cytoplasm are known. One possibility involves the release of peptide from endosomes into the cytosol after cell entry via endocytosis followed by peptide relocation to mitochondria (42). An additional pathway is the direct translocation of peptide across the plasma membrane and subsequent distribution to the mitochondria in response to the mitochondrial membrane potential. A direct transport internalization pathway has been observed in the uptake of selected cell-penetrating peptides including P11LRR (12). Recently, it has also been demonstrated that a group of mitochondrial-penetrating peptides are able to penetrate the plasma membrane in a potential-driven manner (43).

Hence, to probe the possibility of a direct transport of the CAPH dimers across the plasma membrane leading to mitochondrial localization, we first treated the cells with gramicidin, an agent known to depolarize the plasma membrane (44). Interestingly, when MCF-7 cells were pre-treated with gramicidin, followed by incubation with  $2.5 \mu\text{M}$  (P10LRR-ABUA)<sub>2</sub>-C5-G-FL and MitoTracker Red, the CAPH was found to mostly not localize to the mitochondria (Fig. 6). Modulation of the plasma membrane potential, therefore, was found to have a profound effect on

the mode of cell penetration with the dimeric CAPH. Punctuate green fluorescence was still observed for the gramicidin-treated cells, but this staining pattern is likely due to endosomal entrapment of the dimeric CAPH.

The primary function of mitochondria in cellular metabolism is the synthesis of ATP by oxidative phosphorylation via the respiratory chain. This process results in a transmembrane electrochemical gradient, which combines contributions from both a pH difference and membrane potential. In order to study the importance of an intact membrane potential on CAPH dimer mitochondrial localization, MCF-7 cells were treated with FCCP, a selective decoupler of mitochondrial membrane potential. More specifically, cells were first pre-treated with FCCP to depolarize the mitochondrial membrane (45), followed by a 1-h incubation with  $2.5 \mu\text{M}$  of (P10LRR-ABUA)<sub>2</sub>-C5-G-FL, followed by subsequent mitochondrial staining with MitoTracker Red. Consequent confocal fluorescence imaging indicated a noticeable decrease in colocalization between (P10LRR-ABUA)<sub>2</sub>-C5-G-FL and MitoTracker Red in FCCP-treated cells (Fig. 7). This observation indicates a critical role of mitochondrial transmembrane potential in attracting (P10LRR-ABUA)<sub>2</sub>-C5-G-FL to mitochondria.

#### Concentration-Dependent Sub-cellular CAPH Dimer Localization

In the case of the CAPH monomer P11LRR, we previously observed that sub-cellular localization was dependent on

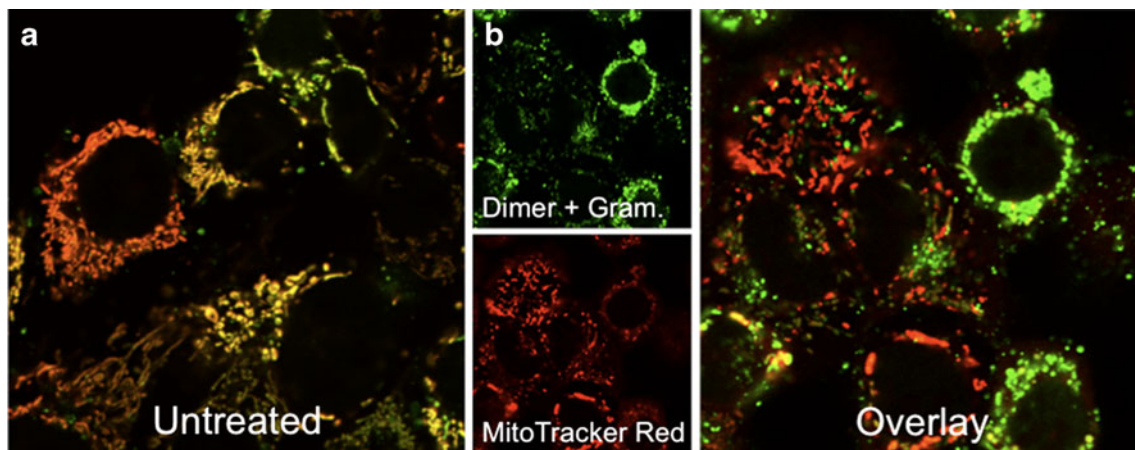


**Fig. 6** (a) MCF-7 cells treated with  $(P10LRR-ABUA)_2-C5-G-FL$  ( $2.5 \mu M$ , 1 h) and MitoTracker Red (Overlay) and (b) cells additionally pre-treated with  $1 \mu M$  Gramicidin for 1 h ( $60\times$  objective with an additional  $3\times$  digital zoom).

the concentration of the CAPH used, with endosomal localization found at concentration below  $10 \mu M$  and mitochondrial localization above  $20 \mu M$  (12). Herein, one of the goals to be achieved through dimerization was to lower the aforementioned concentration threshold for effective mitochondrial targeting. The preceding data is evidence that this threshold can be significantly lowered—direct transport and mitochondrial localization of CAPH dimers were observed at a concentration of  $2.5 \mu M$ . Since concentration-dependent sub-cellular localization was observed in the case of P11LRR, we wanted to investigate if a similar phenomenon could be observed for the CAPH dimer  $(P10LRR-ABUA)_2-C5-G-FL$ . To this end, MCF-7 cells were treated with  $500 \text{ nM}$  of CAPH dimer, and sub-cellular localization was visualized using LysoTracker and MitoTracker stains. Under these conditions the CAPH dimer was found to favor endosomal/lysosomal localization with little localization to the mitochondria, as indicated by the overlay images in Fig. 8. Hence, CAPH dimer cell entry/localization

is also concentration dependent, with endosomal subcellular localization at  $500 \text{ nM}$  and mitochondrial localization from direct transport at  $2.5 \mu M$ . This trend is in agreement with our observations with P11LRR; namely, at  $<10 \mu M$  there was endosomal entry, and at  $>20 \mu M$  there was mitochondrial localization from direct transport, but with a significant reduction in the threshold concentration for CAPH dimer mitochondrial targeting. Interestingly, these data with the CAPH dimer indicate the possibility of further association of CAPH dimers within the membrane.

#### Cellular Viability with CAPH Dimers

The viability of cells that are treated with CAPHs dimers was quantified using the MTT cell viability assay. Specifically, MCF-7 cells were treated with dimeric CAPHs  $(P10LRR-Gly)_2-C5-G-FL$ ,  $(P10LRR-\beta-Ala)_2-C5-G-FL$  and  $(P10LRR-ABUA)_2-C5-G-FL$  at concentrations of 1 and  $5 \mu M$  for 4 h to mimic the conditions used to monitor

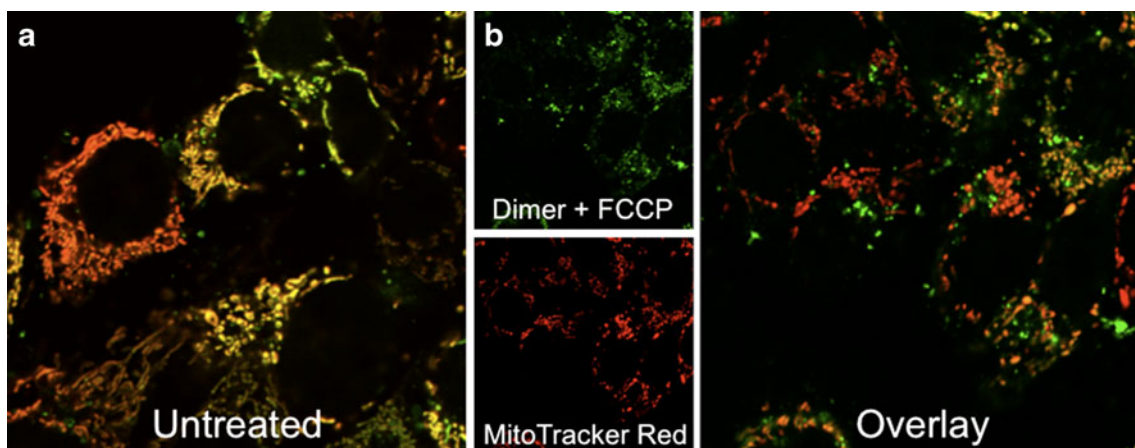


**Fig. 7** (a) MCF-7 cells treated with  $(P10LRR-ABUA)_2-C5-G-FL$  ( $2.5 \mu M$ , 1 h) and MitoTracker Red (Overlay) and (b) cells additionally pre-treated with  $1 \mu M$  FCCP ( $60\times$  objective with an additional  $3\times$  digital zoom).



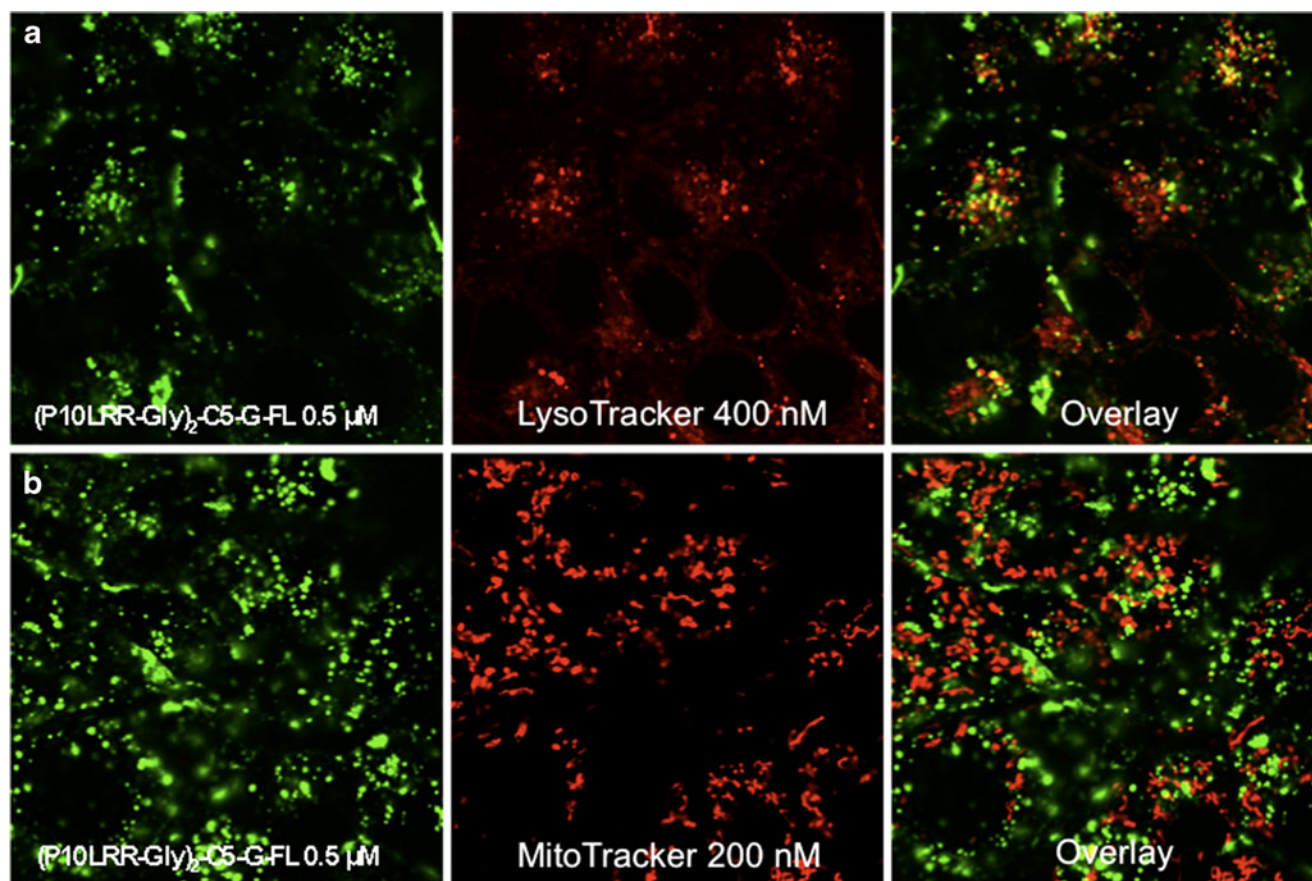


**Fig. 8** (a) MCF-7 cells treated with 500 nM  $(P10LRR-ABUA)_2$ -C5-G-FL and LysoTracker Red (b) MCF-7 cells treated with 500 nM  $(P10LRR-ABUA)_2$ -C5-G-FL and MitoTracker Red (60 $\times$  magnification).

cellular translocation. The cells were found to be fully viable at 1  $\mu$ M with a small decrease in viability at a higher concentration (98, 82 and 85% viable at 5  $\mu$ M, respectively). Since  $(P10LRR-Gly)_2$ -C5-G-FL was the most effective CAPH for cell entry and was also observed to localize to the mitochondria at 2.5  $\mu$ M, its lack of cell toxicity is very promising for future applications.

## CONCLUSION

These data clearly demonstrate that the uptake efficiency of cell-penetrating CAPHs can be noticeably enhanced through dimerization. Also, the dimerized CAPHs were found localized to the mitochondria at a concentration of 2.5  $\mu$ M, a significant decrease in the threshold concentration needed for mitochondrial targeting as compared to monomeric CAPHs. Concentration-dependent studies indicate that the mode of cell penetration may vary between endocytosis and direct transport mechanisms, and modulation of both the plasma and mitochondrial membrane potentials was found to profoundly affect cell

entry and sub-cellular localization, with loss of mitochondrial targeting with loss of both types of membrane potentials. The success of CAPH dimerization in lowering the concentration threshold needed for association with the mitochondria points to the potential of higher order CAPH oligomers as mitochondrial-targeting agents, perhaps with the ability to sequester hydrophobic drugs within a hydrophobic interior. The specific mitochondrial localization and high uptake efficiency of CAPH dimers at relatively low concentrations and low cell toxicity provide many opportunities for targeted drug therapies and encourage further exploration of oligomerization strategies.

## REFERENCES

1. Stewart KM, Horton KL, Kelley SO. Cell-penetrating peptides as delivery vehicles for biology and medicine. *Org Biomol Chem.* 2008;6(13):2242–55.
2. Fillon YA, Anderson JP, Chmielewski J. Cell penetrating agents based on a polyproline helix scaffold. *J Am Chem Soc.* 2005;127(33):11798–803.

3. Potocky TB, Menon AK, Gellman SH. Effects of conformational stability and geometry of guanidinium display on cell entry by beta-peptides. *J Am Chem Soc.* 2005;127(11):3686–7.
4. Geisler I, Chmielewski J. Cationic amphiphilic polyproline helices: side-chain variations and cell-specific internalization. *Chem Biol Drug Des.* 2009;73(1):39–45.
5. Derossi D, Calvet S, Trembleau A, Brunissen A, Chassaing G, Prochiantz A. Cell internalization of the third helix of the Antennapedia homeodomain is receptor-independent. *J Biol Chem.* 1996;271(30):18188–93.
6. Morris MC, Depollier J, Mery J, Heitz F, Divita G. A peptide carrier for the delivery of biologically active proteins into mammalian cells. *Nat Biotechnol.* 2001;19(12):1173–6.
7. Pujals S, Fernandez-Carneado J, Lopez-Iglesias C, Kogan MJ, Giralt E. Mechanistic aspects of CPP-mediated intracellular drug delivery: relevance of CPP self-assembly. *Biochim Biophys Acta.* 2006;1758(3):264–79.
8. Fischer PM, Zhelev NZ, Wang S, Melville JE, Fahraeus R, Lane DP. Structure-activity relationship of truncated and substituted analogues of the intracellular delivery vector Penetratin. *J Pept Res.* 2000;55(2):163–72.
9. Morris MC, Vidal P, Chaloin L, Heitz F, Divita G. A new peptide vector for efficient delivery of oligonucleotides into mammalian cells. *Nucleic Acids Res.* 1997;25(14):2730–6.
10. Pujals S, Fernandez-Carneado J, Ludevid MD, Giralt E. D-SAP: a new, noncytotoxic, and fully protease resistant cell-penetrating peptide. *ChemMedChem.* 2008;3(2):296–301.
11. Jones S, Martel C, Belzacq-Casagrande AS, Brenner C, Howl J. Mitoparan and target-selective chimeric analogues: membrane translocation and intracellular redistribution induces mitochondrial apoptosis. *Biochim Biophys Acta.* 2008;1783(5):849–63.
12. Li L, Geisler I, Chmielewski J, Cheng JX. Cationic amphiphilic polyproline helix P11LRR targets intracellular mitochondria. *J Control Release.* 2009;142(2):259–66.
13. Snyder EL, Dowdy SF. Cell penetrating peptides in drug delivery. *Pharm Res.* 2004;21(3):389–93.
14. Lewin M, Carlesso N, Tung CH, Tang XW, Cory D, Scadden DT, *et al.* Tat peptide-derivatized magnetic nanoparticles allow *in vivo* tracking and recovery of progenitor cells. *Nat Biotechnol.* 2000;18(4):410–4.
15. Lundberg P, Langel U. A brief introduction to cell-penetrating peptides. *J Mol Recognit.* 2003;16(5):227–33.
16. Lindgren M, Hallbrink M, Prochiantz A, Langel U. Cell-penetrating peptides. *Trends Pharmacol Sci.* 2000;21(3):99–103.
17. Ragin AD, Morgan RA, Chmielewski J. Cellular import mediated by nuclear localization signal Peptide sequences. *Chem Biol.* 2002;9(8):943–8.
18. Rothbard JB, Garlington S, Lin Q, Kirschberg T, Kreider E, McGrane PL, *et al.* Conjugation of arginine oligomers to cyclosporin A facilitates topical delivery and inhibition of inflammation. *Nat Med.* 2000;6(11):1253–7.
19. Umezawa N, Gelman MA, Haigis MC, Raines RT, Gellman SH. Translocation of a beta-peptide across cell membranes. *J Am Chem Soc.* 2002;124(3):368–9.
20. Wender PA, Mitchell DJ, Pattabiraman K, Pelkey ET, Steinman L, Rothbard JB. The design, synthesis, and evaluation of molecules that enable or enhance cellular uptake: peptidic molecular transporters. *Proc Natl Acad Sci U S A.* 2000;97(24):13003–8.
21. Singh D, Kiarash R, Kawamura K, LaCasse EC, Garipey J. Penetration and intracellular routing of nucleus-directed peptide-based shuttles (oligomers) in eukaryotic cells. *Biochemistry.* 1998;37(17):5798–809.
22. Wender PA, Rothbard JB, Jessop TC, Kreider EL, Wylie BL. Oligocarbamate molecular transporters: design, synthesis, and biological evaluation of a new class of transporters for drug delivery. *J Am Chem Soc.* 2002;124(45):13382–3.
23. Zhou P, Wang M, Du L, Fisher GW, Waggoner A, Ly DH. Novel binding and efficient cellular uptake of guanidine-based peptide nucleic acids (GPNA). *J Am Chem Soc.* 2003;125(23):6878–9.
24. Geisler I, Chmielewski J. Probing length effects and mechanism of cell penetrating agents mounted on a polyproline helix scaffold. *Bioorg Med Chem Lett.* 2007;17(10):2765–8.
25. Farrera-Sinfreu J, Giralt E, Castel S, Albericio F, Royo M. Cell-penetrating cis-gamma-amino-l-proline-derived peptides. *J Am Chem Soc.* 2005;127(26):9459–68.
26. Torchilin VP. Tat peptide-mediated intracellular delivery of pharmaceutical nanocarriers. *Adv Drug Deliv Rev.* 2008;60(4–5):548–58.
27. Gazit E, Lee WJ, Brey PT, Shai Y. Mode of action of the antibacterial cecropin B2: a spectrofluorometric study. *Biochemistry.* 1994;33(35):10681–92.
28. Matsuzaki K, Murase O, Fujii N, Miyajima K. An antimicrobial peptide, magainin 2, induced rapid flip-flop of phospholipids coupled with pore formation and peptide translocation. *Biochemistry.* 1996;35(35):11361–8.
29. Horobin RW, Trapp S, Weissig V. Mitochondriotropics: a review of their mode of action, and their applications for drug and DNA delivery to mammalian mitochondria. *J Control Release.* 2007;121(3):125–36.
30. Maiti KK, Lee WS, Takeuchi T, Watkins C, Fretz M, Kim DC, *et al.* Guanidine-containing molecular transporters: sorbitol-based transporters show high intracellular selectivity toward mitochondria. *Angew Chem Int Ed Engl.* 2007;46(31):5880–4.
31. Fernandez-Carneado J, Van Gool M, Martos V, Castel S, Prados P, de Mendoza J, *et al.* Highly efficient, nonpeptidic oligoguanidinium vectors that selectively internalize into mitochondria. *J Am Chem Soc.* 2005;127(3):869–74.
32. Rosania GR. Supertargeted chemistry: identifying relationships between molecular structures and their sub-cellular distribution. *Curr Top Med Chem.* 2003;3(6):659–85.
33. Rosania GR, Lee JW, Ding L, Yoon HS, Chang YT. Combinatorial approach to organelle-targeted fluorescent library based on the styryl scaffold. *J Am Chem Soc.* 2003;125(5):1130–1.
34. Johnson JR, Jiang H, Smith BD. Zinc(II)-coordinated oligotyrosine: a new class of cell penetrating peptide. *Bioconj Chem.* 2008;19(5):1033–9.
35. Rudolph C, Plank C, Lausier J, Schillinger U, Muller RH, Rosenecker J. Oligomers of the arginine-rich motif of the HIV-1 TAT protein are capable of transferring plasmid DNA into cells. *J Biol Chem.* 2003;278(13):11411–8.
36. Park SH, Doh J, Park SI, Lim JY, Kim SM, Youn JI, *et al.* Branched oligomerization of cell-permeable peptides markedly enhances the transduction efficiency of adenovirus into mesenchymal stem cells. *Gene Ther.* 2010;17(8):1052–61.
37. Kawamura KS, Sung M, Bolewska-Pedyczak E, Garipey J. Probing the impact of valency on the routing of arginine-rich peptides into eukaryotic cells. *Biochemistry.* 2006;45(4):1116–27.
38. Nishihara M, Perret F, Takeuchi T, Futaki S, Lazar AN, Coleman AW, *et al.* Arginine magic with new counterions up the sleeve. *Org Biomol Chem.* 2005;3(9):1659–69.
39. Brogden KA. Antimicrobial peptides: pore formers or metabolic inhibitors in bacteria? *Nat Rev Microbiol.* 2005;3(3):238–50.
40. Mitchell DJ, Kim DT, Steinman L, Fathman CG, Rothbard JB. Polyarginine enters cells more efficiently than other polycationic homopolymers. *J Pept Res.* 2000;56(5):318–25.
41. Yamashiro DJ, Maxfield FR. Acidification of morphologically distinct endosomes in mutant and wild-type Chinese hamster ovary cells. *J Cell Biol.* 1987;105(6 Pt 1):2723–33.

42. Magzoub M, Pramanik A, Graslund A. Modeling the endosomal escape of cell-penetrating peptides: transmembrane pH gradient driven translocation across phospholipid bilayers. *Biochemistry*. 2005;44(45):14890–7.
43. Horton KL, Stewart KM, Fonseca SB, Guo Q, Kelley SO. Mitochondria-penetrating peptides. *Chem Biol*. 2008;15(4):375–82.
44. Di Virgilio F, Lew PD, Andersson T, Pozzan T. Plasma membrane potential modulates chemotactic peptide-stimulated cytosolic free  $Ca^{2+}$  changes in human neutrophils. *J Biol Chem*. 1987;262(10):4574–9.
45. Ross MF, Da Ros T, Blaikie FH, Prime TA, Porteous CM, Severina II, *et al.* Accumulation of lipophilic dications by mitochondria and cells. *Biochem J*. 2006;400(1):199–208.